Hydrocarbon Chain Ordering in Liquid Crystals Investigated by Means of Infrared Attenuated Total Reflection (IR-ATR) Spectroscopy

U. P. Fringeli *, M. Schadt **, P. Rihak *, and Hs. H. Günthard *

(Z. Naturforsch. **31 a**, 1098–1107 [1976]; received July 8, 1976)

Stationary and modulated IR-ATR spectra of Schiff's base nematic liquid crystals are reported. The mean order parameter of both, the aromatic core and the hydrocarbon chains is determined by analysis of the infrared dichroism of characteristic absorption bands. Hydrocarbon chain ordering was found to be considerably lower than predicted by Marčelja's statistical theory.

1. Introduction

Even-odd alterations of characteristic parameters depending on hydrocarbon chain length such as nematic-isotropic and smectic-isotropic transition temperature, nematic-isotropic transition entropy and core order parameter have been measured [1-3] in homologous series of liquid crystals. The alterations found correspond to the even-odd behaviour of entropy, and melting and boiling temperature of n-parafins.

Recent calculations by Marčelja [4] based on the Maier-Saupe theory [5] take the interactions between hydrocarbon chains as well as those between hydrocarbon chains and aromatic cores of liquid crystals into account. Good agreement between calculated and measured core order parameters was found in homologous series of p-alkoxyazoxybenzenes [3] using Marčelja's theory. However, discrepancies arise between theory and experiment when comparing order parameters of methylene groups in the hydrocarbon chains. Recent studies of deuteron magnetic resonance [6, 7] showed a faster decrease of CH_2-order parameter than should be expected from theory [4] when moving from the rigid core along the hydrocarbon chain.

We shall report on measurements using attenuated total reflection (ATR) infrared spectroscopy to study order parameters of alkyl cyano Schiff' base [8] liquid crystals. Reorientation of the strongly positive dielectric [9] liquid crystal molecules under the influence of electric fields and the consequent changes occurring in the IR-ATR spectra are investigated. Measurements of core order parameter and chain mean order parameter are compared with calculations based on molecular field theory [4]. Our results – which are in good agreement with experimental findings reported by Deloche et al. [6], Emsly et al. [7] and Maier and Englert [10] – show nearly random orientation of the CH_2-groups in the hydrocarbon chains [11]. This finding is contradictory to theoretical predictions made by Marčelja [4].

Reprint requests to Dr. U. P. Fringeli, Laboratory for Physical Chemistry, Swiss Federal Institute of Technology, Universitätsstr. 22, *CH-8006 Zurich*, Switzerland.

* Laboratory for Physical Chemistry, Swiss Federal Institute of Technology Zurich, Switzerland.

** Physics Department F. Hoffmann-La Roche & Co. Ltd., Basle, Switzerland.

2. Experimental

2.1. ATR-Spectra

For a general review of ATR-technique the reader is refered to reference [12].

2.1.1

Stationary ATR spectra were recorded on a Perkin Elmer Mod. 225 infrared spectrometer equipped with two ATR attachments (Wilks Sci. Corp. Mod. 9 and 50). The reflection plates were germanium ($50 \times 20 \times 1$ mm) supplied by Harrick Sci. Corp. The angle of incidence was 30° resulting in about 25 active reflections. Polarization measurements were made using a Perkin Elmer grid polarizer. A schematic diagram of the ATR geometry used is depicted in Figure 1.

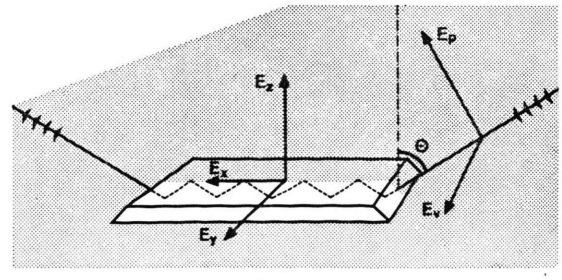

Fig. 1. ATR apparatus. Θ: angle of incidence. E_p, E_v: parallel and perpendicular polarized compounds of the electric field of incident light. E_x, E_y, E_z: electric field components with respect to the coordinate system corresponding to the internal reflection plate ($E_p \rightarrow E_x$, E_z, $E_v \rightarrow E_y$) (Reproduced from Reference [29]).

2.1.2. Modulated Excitation ATR Spectra (ME-ATR)

Several publications have been reported describing the principle of modulation spectroscopy [13]. The technique can always be applied provided the system studied allows periodic excitation. ME-spectroscopy enables selective scanning of those absorption bands of the infrared spectrum resulting from molecules (or parts of them) that are involved in the stimulated processes. All absorption bands which are not affected by excitation are suppressed. The frequency dependence of signal amplitude and phase lag between stimulation and detected infrared signal is typical for the kinetics involved.

Figure 2 shows a diagram of the ATR-spectrometer. A gated 500 Hz sine-wave voltage (1:1 duty

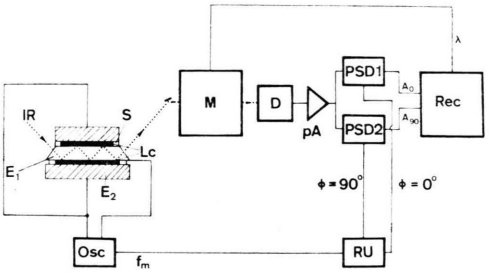

Fig. 2. Modulate Excitation ATR-IR Spectrometer (schematic). IR: Infrared beam; E_1: Electrode 1, germanium internal reflection plate; E_2: Electrode 2, SnO_2 coated glass plate; S: Sample; Osc: Oscillator for stimulation with frequency f_m; M: Monochromator; D: Detector; pA: Preamplifier; PSD1: Phase sensitive detector, tuned to f_m, phase lag $\Phi=0°$ with respect to stimulation; PSD2: Phase sensitive detector, tuned to f_m, phase lag $\Phi=90°$ with respect to stimulation; A_0: DC — component of 0° — channel; A_{90}: DC — component of 90° — channel; λ: Wavelength information from the monochromator; Rec: 2 — channel x-y-recorder; RU: Reference unit.

cycle, 4 Hz frequency, 40 $volts_{pp}$) was used to reorient the liquid crystal molecules in the electric field. For a more detailed description of the apparatus the reader is refered to reference [14].

2.2. Preparation of Liquid Crystal Samples

The long axis of the liquid crystal molecules were aligned parallel to the y-axis (Fig. 1) to get maximum change of polarized ATR-IR-absorption when reorienting the molecules under the influence of an applied electric field. Alignment was initiated by polishing both, the germanium internal reflection plate (electrode E1) and the SnO_2 coated glass plates (electrodes E2) parallel to the y-axis (Figgure 2). Electrodes E1 and E2 were separated by 20 μm mylar spacers. Spontaneous parallel alignment of the liquid crystal molecules occured when filling the electrode sandwiches by capillary action. The homogeneity of molecular alignment could be enhanced by heating up the cells to ~ 10 °C above the nematic-isotropic transition temperature T_c and cooling it slowly down again. Applying a voltage to the electrodes E_1 and E_2 (Fig. 2) caused the long axis of the positive dielectric molecules to realign parallel to the electric field, i.e. parallel to the z-axis.

2.3. Chemicals

The liquid crystal used was RO-TN-200, a mixture of 1 part of 4-(4′-n-propylbenzylidene amino)-benzonitrile and 2 parts of 4-(4′-n-hexylbenzylidene-amino)-benzonitrile with a nematic temperature range of ~ -15 °C to 65 °C. The substance was supplied by F. Hoffmann-La Roche, Ltd., Basel.

3. Results and Discussion

3.1. Assignment of Infrared Absorption Bands

Extensive investigations of liquid crystals using conventional infrared transmission spectroscopy were reported by Maier and Englert [10, 15] and Maier and Markau [16]. The assignment of some prominent absorption bands is listed in Table 1.

It was shown that vibrational coupling between the two benzene rings of the aromatic core of liquid crystal molecules is weak [15]. Therefore, only the local C_{2v} symmetry of one ring has to be considered when estimating the direction of the transition dipole moment. Consequently two directions of transition moments of typical benzene ring vibrations have to be expected, namely parallel and perpendicular to the direction of the para-axis of the aromatic core.

3.2. Molecular Ordering in the Liquid Crystalline State

3.2.1 Stationary ATR-Spectra

Molecular ordering can sensitively be detected by using polarized ATR-spectroscopy (Fig. 1). The reader is refered to reference [17] for a detailed discussion of analysis of polarized spectra.

Liquid crystal molecules are randomly oriented in the isotropic phase above the transition temperature T_c. The spectra in Fig. 3a — recorded at 70 °C $> T_c$ — nevertheless show distinct polarization. This polarization effect is a typical feature of

Table 1. Assignment of some typical infrared absorption bands of RO-TN-200.

Wavenumber [cm^{-1}]	Assignment	Direction of dipole moment relative to para-axis [1]	Remarks
2960	$\nu_{as}(CH_3)$	} weakly polarized [2]	antisymmetric CH_3-stretch
2930	$\nu_{as}(CH_2)$		antisymmetric CH_2-stretch
2871	$\nu_s(CH_3)$		symmetric CH_3-stretch
2858	$\nu_s(CH_2)$	}	symmetric CH_2-stretch
2222	$\nu(C\equiv N)$	∥	
1630	$\nu(C=N)$	22°	
1598	$\nu(C=C)$	∥	skeletal vibration of benzene ring; Ref. [15, 28]
1595	$\nu(C=C)$	⊥	skeletal vibration of benzene ring; Ref. [15, 28]
1495	$\nu(C=C)$	∥	skeletal vibration of benzene ring; Ref. [15, 28]
1465	$\delta(CH_2)$	weakly ⊥ polarized	methylene bending vibration
1418	—	∥	aromatic core. Also present in 4-4′-difluoro-benzalaniline, Ref. [15]
1412	$ev\cdot\delta(CH)$	∥	$-CH=N$-group
1375	$\delta_s(CH_3)$	weakly ∥ polarized	symmetric methyl bending vibr.
1195	$\nu(CX)+\delta(CH)$	∥	stretching of para-substituents X of the benzene ring + CH-deformation, Ref. [15, 28]
1114	$\nu(C-C)+\gamma_t(CH_2)$	weakly ∥ polarized [3]	C—C-stretch of hydrocarbon chains and CH_2-twist [4]
1108	—	⊥	aromatic core

[1] Nematic liquid crystalline state.
[2] Polarization not exactly determinable unless line shape analysis is performed.
[3] Transition dipole moment parallel to hydrocarbon chain in the case of alltrans conformation; Ref. [26, 27]
[4] H—C—C angle deformation (CH_2- and CH_3-groups) in hydrocarbon chain; Ref. [26].

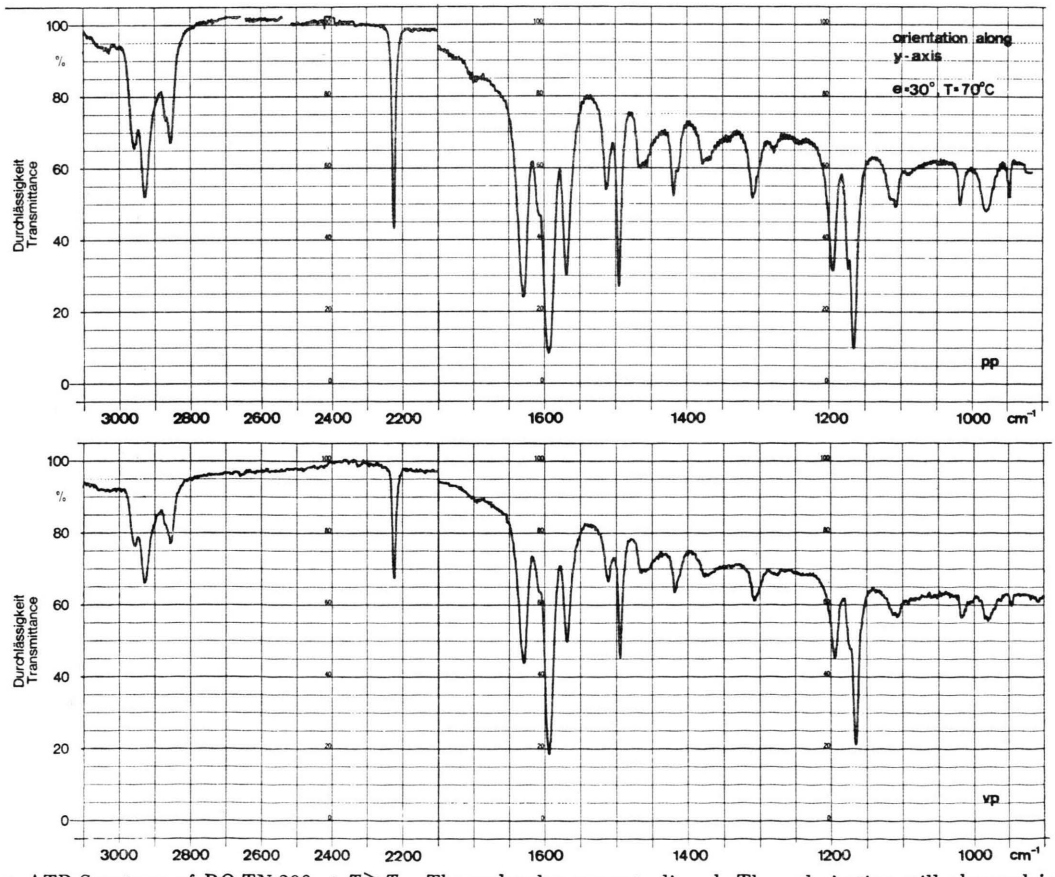

Fig. 3 a. ATR-Spectrum of RO-TN-200 at $T>T_c$. The molecules are not aligned. The polarization still observed is typical for perpendicular (vp) and parallel polarized (pp) ATR-spectra of an isotropic medium. $T_c=64$ °C, $T=70$ °C, $\Theta=30°$.

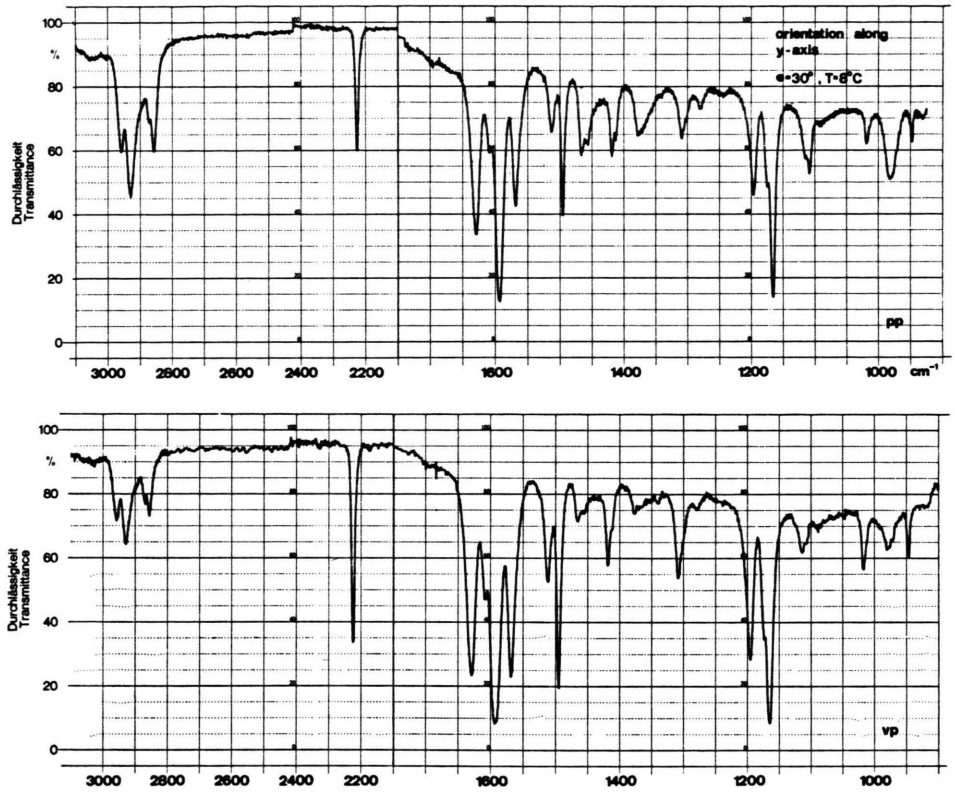

Fig. 3 b. ATR-spectrum of RO-TN-200 at $T<T_c$. The molecules are in the nematic state. The mean orientation of the long axis is parallel to the y-direction of the ATR-reflection plate. This results in a predominant vp-absorption of those vibrations having their main component of transition dipole moment in the y-direction. $T=8$ °C, $\Theta=30°$.

ATR spectroscopy. It originates from the particular field configuration in the rarer medium [12] and has nothing to do with molecular ordering. It has to be taken into account when interpreting ATR spectra.

Two principal groups of absorption bands can be distinguished (Fig. 3 b) in the nematic state of RO-TN-200 ($T_{meas} = 8\ °C < T_c$). (i) Absorption bands showing a strong change in polarization. (ii) Absorption bands showing a very weak change in polarization. The assignment of a number of ATR absorption bands shown in Fig. 3 a and 3 b is given in Table 1. It appears that bands related to aromatic core modes [type (i) bands] are more strongly polarized than bands assigned to typical CH_2-chain vibrations [type (ii) bands]. This finding which is in agreement with results reported by Maier and Englert [10] who qualitatively discussed the spectra of rotational isomers of various alkoxy chains shows that the degree of order of hydrocarbon chains must be very weak in the nematic state.

3.2.2. Modulated Excitation ATR Spectra (ME-ATR)

The dynamic ME-ATR measurements in Fig. 4 show that group (ii) absorption bands are practically absent in the spectra. This finding can be explained in two ways according to Section 2.1. Either the hydrocarbon chains remain stationary and only the polar parts of the molecules move under the reorienting influence of the applied electric field; or also the hydrocarbon chains move but possess a low degree of order, i. e. the isotropic spatial distribution of the oscillating dipoles is not influenced by the orientation process. In both cases no strong absorption bands should occur in the ME-ATR spectrum (Figure 4). However, from stationary measurements it must be concluded that only the latter case can be true. This is shown by unmodulated ATR-spectra depicted in Figure 3 a, 3 b and 5.

The measurements of Fig. 5 were made using the propyl and hexyl components of RO-TN-200, respec-

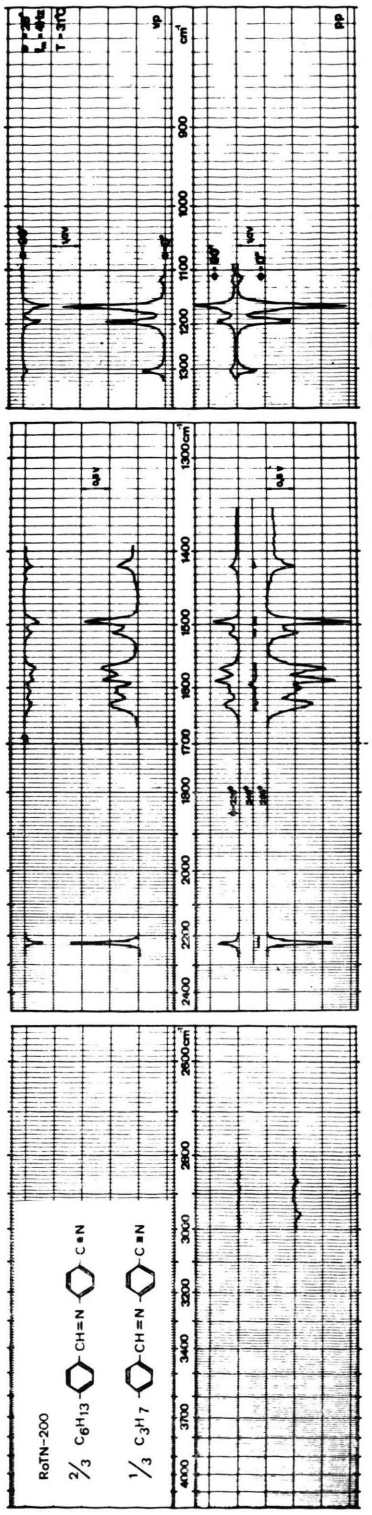

Fig. 4. Modulation spectrum of RO-TN-200. vp: Perpendicularly polarized; pp: Parallel polarized; $\Phi = 0°$: Signal component with 0° phase lag with respect to stimulation; $\Phi = 90°$: Signal component with 90° phase lag with respect to stimulation. The weak modulation signals in the 3000 cm^{-1} region result from the CH_3-group of the propyl-component. The intensity of an absorption band is proportional to the corresponding modulated amount of the absorption coefficient ($A = -\ln T$).

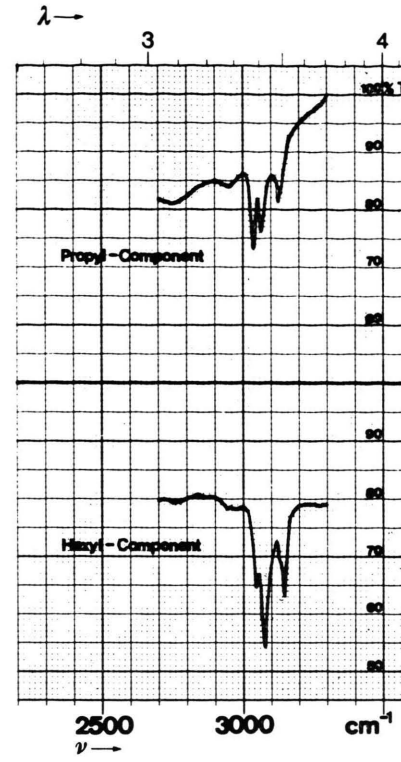

Fig. 5. Stationary ATR-spectrum of propyl and hexyl component of RO-TN-200 in the CH-stretching region.

tively. They show (Fig. 5) that the absorption coefficients of $\nu_a(CH_3)$ and $\nu_s(CH_3)$ are significantly larger than the corresponding absorption coefficients of CH_2-group vibrations. A comparison of the band contour in the CH-stretching region of the ME-ATR spectrum (Fig. 4) with the measurements of Fig. 5 leads to the conclusion that the $\nu(CH)$-absorption bands in the ME-sepctrum are due to the propyl component of RO-TN-200. Therefore, the methyl group in C-3 position has a small degree of order thus producing only small changes of polarized absorption when reorientation of the molecules induced by an externally applied electric field occurs.

No significant contribution of the methyl group in the hexyl component of RO-TN-200 was found (Figure 5). Otherwise, the $\nu(CH_2)$-vibrations at 2930 and 2858 cm^{-1} would have been more prominent. This leads to the conclusion that the degree of order along the hydrocarbon chain decreases very rapidly, a finding which is in agreement with recent NMR studies [6, 7].

The dynamics of molecular alignment can be investigated by measuring the frequency dependence of signal amplitude and phase angle Φ between stimulating and detected signal using ME-ATR spectroscopy [13] (Section 2.1.2). Φ can easily be calculated from $\mathrm{tg}\,\Phi = A_{90}/A_0$ where A_{90} and A_0 denote the absorption coefficients measured in the 90° and 0° phase channels, respectively. A detailed kinetic analysis will be published later.

3.2.3. Measurements of the Molecular Orientation

Molecular ordering is discussed in terms of distribution functions of aromatic cores and hydrocarbon chains. In case of liquid crystals a distribu tion function $f(\gamma)$ for axial orientation is required where γ denotes the angle between the direction of orientation (y-axis) and the para-axis of the molecules. $f(\gamma)\,\mathrm{d}\gamma$ is proportional to the number of para-axis pointing into the conical element with symmetric angle $\gamma, \gamma + \mathrm{d}\gamma$. (The reader is refered to Ref. [17] for a detailed discussion of molecular orientation.)

The simplest molecular distribution can be described by the delta function.

$$f(\gamma) = \delta(\gamma - \gamma_0) \tag{1}$$

which means that all para-axis are oriented at a fixed angle γ_0 with respect to the y-axis. However, this type of distribution function is not realistic in cases where the degree of order is as low as in the hydrocarbon chains of liquid crystals. Therefore we used the Kratky distribution function [17, 18] describing the orientation changes occuring in polymers when exerting a force upon them. The model assumes that polymer chain segments are randomly oriented as long as the polymer is not stretched. In the unstretched state a volume element of side length L' is defined which changes its length from L' to L when stretching occurs in a direction parallel to L'. The stretching ratio v is defined as

$$v = L/L' .$$

Random distribution is characterized by $v = 1$; whereas $v = \infty$ characterizes perfect ordering along the direction of stretching.

In our case parallel alignment of the liquid crystal molecules was achieved by polishing the electrode surfaces. In analogy to polymer orientation the parameter v in the Kratky distribution function can be used as as measure for the quality of surface alignment of the liquid crystal molecules. The Kratky distribution function is defined as [18]

$$f(\gamma) = \frac{v^{3/4} \sin\gamma}{(v^{-3/2}\cos^2\gamma + v^{3/2}\sin^2\gamma)^{3/2}} . \tag{2}$$

Calculation of the Parameter v

Polarized infrared spectra enable direct determination of the dichroic ratio R defined by

$$R = A_{\mathrm{pp}}/A_{\mathrm{vp}} , \tag{3}$$

where A_{pp} and A_{vp} denote the absorption coefficients with respect to parallel (pp) and perpendicular (vp) polarization, respectively. Knowing R, v can be determined in a straight forward way [17]. However, it must be noted that the calculations in Ref. [17] were made for transmission measurements where all infrared electric field components are equal which is not the case for ATR measurements where the electric field is inhomogenious (c.f. 3.2.1).

In our experiments the molecules are spontaneously aligned along the y-axis. The ATR dichroic ratio is then given by

$$R^{\mathrm{ATR}} = R^{\mathrm{T}}(E_x^2 + E_z^2)/E_y^2 \tag{4}$$

where R^{T} is the transmission dichroic ratio (reduced dichroic ratio). For uniaxial orientation R^{T} is given by [17]

$$R^{\mathrm{T}} = (\sin^2\Theta + S')/(2\cos^2\Theta + S') \tag{5}$$

where Θ denotes the angle between transition dipole moment and para-axis of the molecule. S' is the order parameter defined by

$$S' = \frac{\int_0^{\pi/2} \sin^2\gamma\, f(\gamma)\,\mathrm{d}\gamma}{1 - \frac{3}{2}\int_0^{\pi/2} \sin^2\gamma\, f(\gamma)\,\mathrm{d}\gamma} . \tag{6}$$

S' is different from the order parameter S commonly used in NMR and EPR spectroscopy. However, S is related to S' by expression (7)

$$S = \tfrac{3}{2}\int_0^{\pi/2} \cos^2\gamma\, f(\gamma)\,\mathrm{d}\gamma - \tfrac{1}{2} = 1 - \tfrac{3}{2}S'/(1 + \tfrac{3}{2}S') . \tag{7}$$

Therefore, once R^{ATR} has been determined S' can be calculated using Eqs. (4) and (5). v can be determined from Eqs. (2) and (6), i.e. from plotting S' versus v (c.f. Ref. [17]). The experimental data used for the calculations are listed in Table 2

while the Kratky distribution functions of the aromatic core and the hydrocarbon chains as well as the corresponding integrals are plotted in Figure 6.

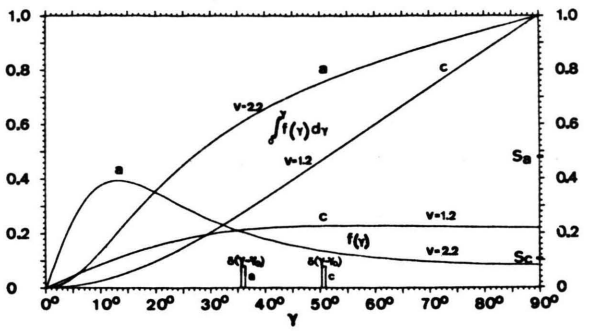

Fig. 6. Kratky distribution functions (2) for aromatic core (a) and methylene groups (c) *. $\int_0^{\gamma} f(\gamma)\,d\gamma$ denotes the fractional number of core axis (a) and methylene groups (c) * respectively, pointing into the cone with angle γ. S_a and S_c are the corresponding order parameters, c.f. (7). $\delta_a(\gamma-\gamma_0)$ and $\delta_c(\gamma-\gamma_0)$ denote the corresponding delta distribution functions, c.f. (1).

3.3. Statistical Calculation of Hydrocarbon Chain Ordering

The mean dichroic rations of $\delta_s(CH_3)$, $\delta(CH_2)$ and $\nu_a(CH_2)$ of hexyl chains in RO-TN-200 were calculated by means of Marčelja's theory [4]. The ATR-dichroic ratio in terms of the 3 components of the transition dipole moment M_x, M_y and M_z is given by

$$R^{ATR} = \frac{E_x^2\langle M_x^2\rangle + E_z^2\langle M_z^2\rangle}{E_y^2\langle M_y^2\rangle}. \qquad (8)$$

Assuming cylindrical symmetry about the y-axis R^{ATR} is given by

$$R^{ATR} = \frac{1}{2}\,\frac{E_x^2+E_z^2}{E_y^2}\cdot\frac{\langle M_x^2\rangle + \langle M_z^2\rangle}{\langle M_y^2\rangle}$$

where

$$\langle M^2\rangle = \frac{1}{Z}\int_0^{\pi/2}\int_0^{2\pi}\sum_{\substack{\text{all}\\ \text{conf. } i}} M_i^2\, e^{-E_i/RT} f(\gamma)\,d\varphi\,d\gamma \quad \text{is}$$

the statistical average of the squared component of the transition dipole moment (summed over all conformations). Z is the corresponding partition function and M_i the component of the transition moment corresponding to the i-th chain conformation having the potential energy E_i. $f(\gamma)$ denotes the axial distribution function introduced in Sect. 3.2., Equation (2). γ and φ are the polar angles specifing the orientation of the C_0-C_1 bond (para-axis).

In case of methylene vibrations $\delta(CH_2)$ and $\nu_a(CH_2)$ it was assumed that

$$M_i^2 = \sum_j M_{ij}^2,$$

where M_{ij} is the component of the transition dipole moment corresponding to the j-th methylene group in the i-th chain conformation. Summation extends over all methylene groups in the chain. The transition dipole moments considered here are assumed to be oriented in the following way:

$\boldsymbol{M}[\delta_s(CH_3)]$	parallel to the C_3-symmetry axis of the methyl group;
$\boldsymbol{M}[\delta(CH_2)]$	parallel to the bisectrix of the HCH-angle;
$\boldsymbol{M}[\nu_a(CH_2)]$	parallel to the line connecting the two corresponding H atoms.

The order parameter S_j of the j-th methylene group is defined by [4]

$$S_j = \tfrac{3}{2}\cos^2\vartheta_j - \tfrac{1}{2},$$

where ϑ_j is the angle between the normal to the HCH plane and the director which is in our case parallel to the y-axis of the coordinate system (Figure 1). The mean order parameters S_c of the hydrocarbon chain is then defined by

$$S_c = \frac{1}{N}\sum_{i=1}^{N}\langle S_i\rangle \qquad (9)$$
$$= \frac{1}{NZ}\sum_{i=1}^{N}\int_0^{\pi/2}\int_0^{2\pi} f(\vartheta)\sum_{\text{all conf.}} S_{ik}\exp\{-E_k/RT\}\,d\varphi\,d\vartheta;$$

$N=5$, number of methylene groups.

The potential energy of the chain is composed of two parts [4]

$$E = E_{int} + E_{ext}.$$

E_{int} denotes the internal energy of the alkyl chain in which three successive C–C bonds can assume either trans (t), gauche + (g+) or gauche − (g−) conformation. Assuming nearest neighbour interaction between chain segments the internal energy of a C_6-chain becomes

$$E_{int} = \sum_{i=2}^{5} E(\xi_i, \xi_{i-1}),$$

ξ stands for t, g^+ or g^-, respectively. The rotational barriers taken from Ref. [4] are $E(\xi, t) = 0, E(t, g^{\pm})$

* normals to the H–C–H-plane.

Table 2. Mean values of R^{ATR}: ATR dichroic ratio, c.f. (3); R^T: Reduced dichroic ratio, c.f. (4), (5); Θ: Angle between transition dipole moment and long axis of the aromatic core (para-axis); S': Order parameter calculated from (5); v: Extension ratio of Kratky function (2) calculated from (6); S: Order parameter calculated from (7).

Vibration Symbol	cm^{-1}	R^{ATR}	R^T [1]	Θ	S'	v	S	Remarks
$\nu_{as}(CH_2)$	2930	1.95 [2]	1.04 ± 0.10	$\sim 90°$ [3]	6.9 — ∞	1.15—1.00	0.088—0	Hydrocarbon chain
$\nu_s(CH_2)$	2858	1.92 [2]	1.03 ± 0.10	$\sim 90°$ [3]	7.5 — ∞	1.14—1.00	0.082—0	$S' = 5.2$
$\delta(CH_2)$	1465	2.20	1.18 ± 0.06	$\sim 90°$ [3]	4.2 — 8.3	1.24—1.13	0.137—0.074	$v = 1.2$
$\delta_s(CH_3)$	1375	1.65	0.88 ± 0.07	$\sim 35°$ [3]	4.1 —17.4	1.25—1.07	0.140—0.037	$S = 0.11$
$\nu(C-C)$	1114	1.34 [4]	0.72 ± 0.035	$\sim 0°$ [3]	4.3 — 6.2	1.23—1.18	0.134—0.097	are selected mean values, c.f. Fig. 6
$\nu(C \equiv N)$	2222	0.48	0.257 ± 0.005	0°	0.68— 0.72	2.2 —2.25	0.495—0.480	aromatic core $S' = 0.71$ $v = 2.2$
$\nu(C=N)$	1630	0.70	0.374	22° [5]	—	—	—	$S = 0.485$ are selected mean values, c.f. Fig. 6

[1] Calculated from R^{ATR} by means of (4). $E_x^2/E_y^2 + E_z^2/E_y^2 = 1.87$ was calculated following Reference [12]. The refractive indices of RO-TN-200 are: $n'' = 1.82$ and $n' = 1.55$ respectively.
[2] Estimated values. No band shape analysis was performed.
[3] In order to minimize steric hinderance mean orientation of the hydrocarbon chains was assumed parallel to the para-axis.
[4] Determined by means of band shape analysis, $\Delta\nu_{1/2} = 6.5\ cm^{-1}$. The second band was found to be at $1108\ cm^{-1}$ with $\Delta\nu_{1/2} = 2.5\ cm^{-1}$ and $R^{ATR} = 5.3$.
[5] Calculated angle between the transition moment of $\nu(C=N)$ and the para-axis by means of Equation (5).

$= E(g^{\pm}, g^{\pm}) = 400$ cal/mol and $E(g^{\pm}, g^{\mp}) = 2200$ cal/mol.

E_{ext} denotes the energy of the chain in the mean molecular field of the nematic phase. In analogy to Ref. [4] E_{ext} becomes

$$E_{ext} = -(2 C_c S_c V_{cc} + C_a S_a V_{ca}) \sum_{i=1}^{N} S_i . \quad (10)$$

The subscripts a and c stand for aromatic rings and chains, respectively, C_a and C_c are the corresponding volume fractions, S_a and S_c denote the mean order parameters. For 4-(4′-n-hexyl-benzylidene amino)-benzonitrile the volume fractions as estimated from a molecular model were taken as $C_c = 0.36$ and $C_a = 0.64$, respectively. S_a is 0.48 according to Table 2. The constant V_{cc} describing the energy of a chain segment in the field of the other chains is estimated [4] to be 680 cal/mol. V_{ca} denotes the energy of a chain segment in the field of the aromatic cores, it is the only adjustable parameter in Marčelja's theory [4]. The factor 2 is included to normalize the values of S_c between zero and one for the disordered and the all-trans ordered state, respectively.

The values of the order parameters S_i, S_a, S_c and of the dichroic ratio R^{ATR} of the three group vibrations may now be obtained as self consistent solutions of Eqs. (8), (9) and (10). The results of our calculations are summarized in Table 3.

Table 3. Values of order parameters S_i, mean order parameter S_c of hydrocarbon chains and ATR dichroic ratios calculated for different constants V_{cc} and V_{ca} at $T = 8$ °C.

V_{cc} (cal/mol)	680	680	680	400	200	50	680	0
V_{ca} (cal/mol)	500	100	50	50	50	50	0	0
S_1	0.456	0.311	0.293	0.270	0.260	0.254	0.276	0.243
S_2	0.385	0.145	0.115	0.077	0.059	0.049	0.086	0.032
S_3	0.394	0.150	0.119	0.080	0.062	0.052	0.089	0.034
S_4	0.343	0.094	0.064	0.026	0.009	0.000	0.035	–.018
S_5	0.304	0.113	0.090	0.060	0.046	0.039	0.067	0.025
S_c	0.376	0.163	0.136	0.103	0.087	0.079	0.111	0.063
$R^{ATR}(\delta(CH_2))$ [2]	2.76	2.09	2.02	1.95	1.92	1.90	1.96	1.87
$R^{ATR}(\nu_{as}(CH_2))$	4.82	2.83	2.67	2.48	2.39	2.36	2.53	2.27
$R^{ATR}(\delta_s(CH_3))$	2.37	2.53	2.55	2.57	2.58	2.58	2.56	2.59

[1] For a detailed description of the applied procedure leading to these results the reader is refered to Reference [25].
[2] The ratio of the ATR electric field components $(E_x^2 + E_z^2)/E_y^2 = 1.87$ involved in R^{ATR} [c.f. (8)] was calculated from Harrick [12].

4. Remarks and Conclusions

4.1. Boundary Layer

The mean penetration depth d_p of IR-ATR light into the liquid crystal is calculated[12] to be $d_p = 0.42$ to 1.41 microns in the wavelength range $\lambda = 3$ to 10 microns for an angle of incidence $\Theta^{ATR} = 30^\circ$ and a ratio of refractive indeces $\bar{n}_{LC}/n_{Ge} = 0.413$. $\bar{n}_{LC}$ = average refractive index of liquid crystal, n_{Ge} = refractive index of germanium. The spectra depicted in Sect. 3 are therefore related to a thin boundary layer of liquid crystal molecules at the germanium-liquid crystal interface.

4.2. Polarization of Absorption Bands

The assignment of infrared absorption bands of benzalaniline (which is identical with the aromatic core of RO-TN-200) is reported[15] in a previous infrared study on liquid crystals. Number and intensity of absorption bands with polarization parallel and perpendicular to the molecular axis are about the same[15]. However, in our spectra (Figs. 3, 4) it is found that practically all intense absorption bands belong to vibrations polarized more or less parallel to the para-axis. This may be due to the strong dielectric anisotropy $\Delta\varepsilon = \varepsilon_{\parallel} - \varepsilon_{\perp} = +18.3$ of RO-TN-200[19] compared with $\Delta\varepsilon < 0$ of benzalaniline

4.3. Overlapping of Absorption Bands

In order to determine the dichroic ratio R^{ATR} it is necessary to know the integral- or the peak absorption coefficients[20] along both polarizations, parallel and perpendicular, respectively. Since many absorption bands of interest are overlapped by other bands, line shape analysis is a prerequisite for an accurate determination of the dichroic ratio.

Line shape analysis was carried out to determine the dichroic ratio of the 1114 cm^{-1} absorption band (Fig. 3) which could be assigned to $\nu(C-C)$, c.f. Table 1 and 2. The dichroic ratio of the second band in the doublett (Fig. 3) was determined to be $R^{ATR} = 5.3$, with $\Delta\nu_{1/2} = 2.5$ cm^{-1}. Therefore, it must be assigned to a vibration of the aromatic core which is perpendiculary polarized with respect to the long molecular axis. Line shape analysis in the region of $\delta_s(CH_3)$ and $\delta(CH_2)$ is not necessarly required because the dichroic ratios of the overlapping bands [e.g. $\delta_{as}(CH_3)$ at 1456 cm^{-1}] are approximately the same as those of the bands of interest.

4.4. Comparison of Calculated an Experimentally Determined Dichroic Ratios

In Table 3 (bottom) the mean dichroic ratios of typical hydrocarbon chain vibrations are listed as a function of the molecular field coupling constants V_{cc} and V_{ca}. The set $V_{cc} = 680$ cal/mol and $V_{ca} = 472$ cal/mol (left) was used by Marčelja[4]. The case for no coupling $V_{cc} = V_{ca} = 0$ is listed on the right hand side. Comparing Table 3 with Table 2 and Fig. 6 leads to the conclusion that V_{ca} must be expected to be about 10 times smaller than proposed in Ref.[4] to get a value for the mean order parameter which is in satisfactory agreement with the experimentally determined $S_c = 0.11$. This result is in agreement with recent theoretical considerations[21]. In addition to the above the coupling constant V_{cc} turned out to be rather unspecific.

There still remains a discrepancy between the calculated and experimentally determined dichroic ratios, especially so with respect to the symmetric methyl bending vibration $\delta_s(CH_3)$, see Table 2 and 3. From the calculated values of $R^{ATR}(\delta_s(CH_3))$ it must be concluded that the transition moment of $\delta_s(CH_3)$, expected to lie parallel to the direction of the last C – C-bond, exhibits a significant polarization perpendicular to the para-axis. However, the experimental value of $R^{ATR}(\delta_s(CH_3))$ results in a slight polarization parallel to the molecular axis. A plausible explanation for this discrepancy could be steric hinderance which is expected to become significant for molecules in the liquid crystalline environment-whereas the calculated data in Table 3 are derived from the isolated molecule.

Finally it should be mentioned that $R^{ATR}(\delta_s(CH_3))$ of the hexyl component is somewhat higher than the experimentally determined value in Table 2. This is due to RO-TN-200 containing 33% n-propyl Schiff'-base whose methyl group exhibits a higher order parameter than that of the hexyl component (c.f. Sec. 3.2.2). The experimentally determined dichroic ratio will nevertheless remain significantly lower than the calculated ratio.

4.5. Application of Molecular Field Theory to Biological Systems

Based on his liquid crystal results[4] Marčelja extended his theory to calculate the conformation of hydrocarbon chains in oriented lipid bilayers and to determine the pressure-area diagrams of spread

monolayers [22]. His theory was also used to determine hydrocarbon chain conformations in systems of lipid multilayers [23] as well as to study the influence of proteins on the conformation of the hydrocarbon chains of surrounding lipids [24].

Although very good agreement between calculated and experimental results is reported in Refs. [3, 4, 22, 23] it should be recognized that Marčelja's theory [4] is not fully consistent in view of our experimental findings as well as of those published recently by others [6, 7, 10, 21]. Marčelja's theory reproduces correctly the even odd effect of transition temperature, transition entropie and core-order-parameters of a homolgous serie of liquid crystals, however, it can not correctly reproduce order parameters and dichroic ratios of hydrocarbon chains when using the same set of parameter as for the core-order calculations.

Acknowledgement

The authors wish to thank Mrs. M. Fringeli for technical assistance. Financial support by the Swiss National Foundation (project No. 3.0570.73 and No. 3.521-0.75) and by the F. Hoffmann-La Roche Foundation (project No. 127) is gratefully acknowledged.

[1] H. Arnold, Z. Phys. Chem. Leipzig **226**, 146 [1964].
[2] J. van der Veen, W. H. de Jan, M. W. M. Wanninkhof, and C. A. M. Tienhoven, J. Phys. Chem. **77**, 2153 [1973].
[3] A. Pines, D. J. Ruben, and S. Allison, Phys. Rev. Letters **33**, 1002 [1974].
[4] S. Marčelja, J. Chem. Phys. **60**, 3599 [1974].
[5] W. Maier and A. Saupe, Z. Naturforsch. **A14**, 882 [1959]; **A15**, 287 [1960].
[6] B. Deloche, J. Charvolin, L. Liébert, and L. Strzelecki, Journal de Physique **36**, C1–C20 [1975].
[7] J. W. Emsly, J. C. Lindon, and G. R. Luckhurst, Molecular Physics **30**, 191 [1975].
[8] A. Boller and H. Scherrer, German Offenlegungsschrift Nr. 2 306 738 [1973].
[9] M. Schadt, J. Chem. Phys. **56**, 1494 [1972].
[10] W. Meier and G. Englert, Z. Phys. Chem. NF **19**, 168 [1959].
[11] U. P. Fringeli, M. Schadt, and Hs. H. Günthard, V^th Biophysics Congress Copenhagen 1975.
[12] N. J. Harrick, "Internal Reflection Spectroscopy", Interscience Publishers, New York 1967.
[13] R. M. Hexter, J. Opt. Soc. Amer. **53**, 703 [1963]; H. S. Johnston, G. E. Graw, T. T. Paukert, L. W. Richards, and T. van den Bogaerde, Proc. Nat. Acad. Sci., USA **52**, 1146 [1967]; U. P. Fringeli, Thesis Nr. 4366, ETH-Zurich [1969]; U. P. Fringeli and Hs. H. Günthard, Appl. Optics **10**, 819 [1971]; M. Forster, K. Loth, M. Andrist, U. P. Fringeli, and Hs. H. Günthard, Chem. Phys., in the press.
[14] U. P. Fringeli, W. Münch, and Hs. H. Günthard, J. Phys. E: Sci. Instrum. to be published.
[15] W. Maier and G. Englert, Z. Elektrochem. Ber. Bunsenges. Physik. Chem. **62**, 1020 [1958]; Z. Elektrochem. Ber. Bunsenges. Physik. Chem. **64**, 689 [1960].
[16] W. Maier and K. Markau, Z. Physik. Chem. NF **28**, 190 [1961].
[17] R. Zbinden, Infrared Spectroscopy of High Polymers, Acad. Press, London 1964.
[18] O. Kratky, Kolloid-Z. **64**, 213 [1933].
[19] M. Schadt and C. von Planta, J. Chem. Phys. **63**, 4379 [1975].
[20] R. D. B. Fraser, J. Chem. Phys. **21**, 1511 [1953].
[21] A. Wulf, J. Chem. Phys. **64**, 104 [1976].
[22] S. Marčelja, Biochim. Biophys. Acta **367**, 165 [1974].
[23] H. Schindler and J. Seelig, Biochemistry **14**, 2283 [1975].
[24] S. Marčelja, V^th Biophysics Congress, Copenhagen 1975.
[25] P. Rihak, U. P. Fringeli, and Hs. H. Günthard, to be published.
[26] J. H. Schachtschneider and R. G. Snyder, Spectrochim. Acta **19**, 117 [1963].
[27] G. Herzberg, Molecular Spectra and Molecular Structure, Van Nostrand Company, Amsterdam 1945.
[28] K. W. F. Kohlrausch, Acad. Verlagsges., Leipzig 1943.
[29] F. Kopp, U. P. Fringeli, K. Mühlethaler, and Hs. H. Günthard, Biophys. Struct. Mechanism **1**, 75 [1975].